Electrical Behaviour of Magnetic Nickel Nanoparticles Encapsulated in Silica

S. Sujatha and E. Thirumal

Research Journal of Agricultural Sciences
An International Journal

P- ISSN: 0976-1675
E- ISSN: 2249-4538

Volume: 13
Issue: 06

Res. Jr. of Agril. Sci. (2022) 13: 1881–1885

CARAS

Res. Jr. of Agril. Sci. (Nov-Dec 2022)
13(6): 1881–1885

ISSN: 0976-1675 (P)
ISSN: 2249-4538 (E)

www.rjas.org

Full Length Research Article

Electrical Behaviour of Magnetic Nickel Nanoparticles Encapsulated in Silica

S. Sujatha[1] and E. Thirumal*[2]

Received: 27 Sep 2022 | Revised accepted: 29 Nov 2022 | Published online: 22 Dec 2022

A B S T R A C T

Nanocrystalline Ni particles were synthesized by chemical reduction and coated with silica layer by a modified Stöber process. X-ray diffraction patterns of the samples showed an average size of 18 nm for the Ni nanocrystals. The coated particles exhibited improved thermal stability. The magnetic hysteresis established the ferromagnetic behaviour and an increased coercivity for the nanocomposite. The impedance measurement showed activation energy of 1.3 eV and decrease in dc conductivity with temperature. The high dielectric constant over a wide frequency range is explained as a consequence of concentration of Ni much higher than the percolation threshold. The conductivity mechanism is dominated by tunneling at low frequency and electron hopping at high frequencies. The material suffers a low loss in high frequency range, making it suitable for high frequency magnetic applications.

***Key words*:** Nickel, Oxidation, Thermal properties, Silica, Metal-insulator transitions, Electrical measurements

Nickel nanoforms attract continuing interest with their magnetic [1-2], optical [3-4], field emission [5], mechanical [6] and catalytic [7-9] properties. Nanocomposites of nickel with silica [10], carbon [11], polymer [12] and CNT [13] have been investigated for various applications. Nickel-silica nanocomposites have been obtained as Ni-embedded silica [14-17] and as core-shell structures with nickel at core [18-20] or as shell [21]. Ni/SiO_2 nanocomposites have been shown to exhibit magneto-optical [15], magnetic [22] and electrical [16], [20], [22] properties. In general, suitable encapsulation of nanoparticles is often preferred in nanotechnology in order to prevent grain growth or agglomeration and gain protection against oxidative or corrosive environments by surface passivation. In the case of ferromagnetic metal nanoparticles, their core-shell nanocomposites with the insulating silica further enhance their application potential by modification of their properties. For example, nanocrystalline Ni despite its very good soft ferromagnetic properties and high Curie temperatures is not useful for high frequency magnetic applications due to unacceptably large eddy current losses. Silica coating of individual nanoparticles offer several advantages by protecting them against oxidative degradation and agglomeration and also increasing the resistivity several folds thus making them useful for high frequency magnetic devices.

* **E. Thirumal**
✉ esthirumal@gmail.com

[1-2] Department of Physics, Faculty of Arts and Science, Bharath Institute of Higher Education and Research, Chennai - 600 073, Tamil Nadu, India

Core-shell nanocomposite with metal nanoparticle as core and an amorphous silica layer as shell has been prepared in earlier reports using tetraethyl orthosilicate (TEOS) as silica source by sol-gel routes [20] or adhesion method [18]. In this paper, we report the preparation of Ni nanoparticles, its subsequent surface coating with silica and investigations on the magnetic and electric properties of the composite.

MATERIALS AND METHODS

The nanocrystalline Ni powder was prepared by a hydrazine reduction method. Commercially available reagents of analytical grade were used without further purification in this synthesis. Typically, an aqueous solution of 0.2 M / 100 ml was first prepared by dissolving the precursor nickel chloride in water containing trace acetone (1 ml). Then, hydrazine hydrate solution (1 M, 5 ml) and NaOH solution in trace quantity (1 M, 2 ml) were added in sequence, following an earlier procedure [23-24]. Precipitation of ultrafine nickel particles was completed after 2 h on maintaining the reaction at 333 K. The black precipitate was recovered after repeated washing with double distilled water and ethanol. The synthetic Ni nanoparticles were annealed in air at 473, 573 and 673 K for 1 hour.

The silica coating of the Ni particles was carried out by hydrolysis of TEOS and its subsequent condensation as in Stöber process [25]. In order to prepare the Ni/SiO_2 nanocomposite, the as-prepared Ni nanoparticles were re-dispersed in 25 ml of 4.2 vol% of ammonia (28% NH_3 in H_2O) in ethanol and immediately 25 ml of 10 vol% TEOS in ethanol was added slowly under vigorous stirring for 24 h and the product was then aged for 48 h. The resulting Ni/SiO_2

nanocomposite powder was washed with acetone and dried by flash heating at 333 K. Portions of Ni/SiO_2 nanocomposite powder were also annealed in air at temperatures of 573, 673, 773 and 873 K for 2 h.

The phase and microstructure of samples were characterized by X-ray Diffraction (XRD) using Cu-Kα_1 radiation on a high-resolution diffractometer from Huber Diffraktionstechnik. Magnetization measurements were carried out with an applied field up to 7 kOe on a EG&G Princeton applied research 4500 vibrating sample magnetometer (VSM). Impedance characteristics in the frequency range of 1 Hz – 10 MHz were obtained for pellets of as-prepared and annealed Ni/SiO_2 powders using a Solartron SI 1260 impedance/gain phase analyzer. These experiments were also carried out for the as-prepared samples at temperatures from room temperature upto 363 K in steps of 10 K in normal atmosphere.

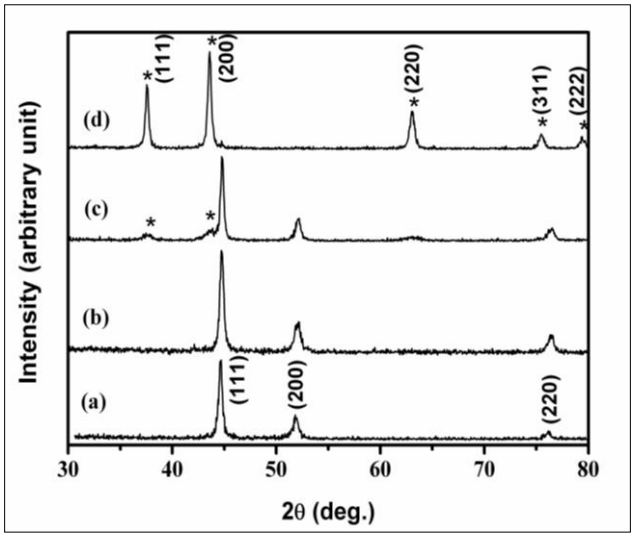

Fig 1 X-ray diffraction patterns of (a) as-prepared Ni powder and annealed at (b) 473 K, (c) 573 K and (d) 673 K for an hour (in air). ∗-indicates the peaks corresponding to fcc- NiO

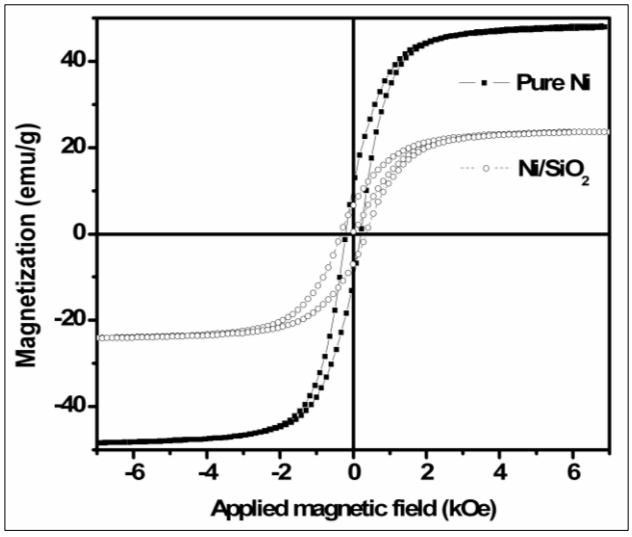

Fig 3 Hysteresis loops for as-prepared Ni and Ni/SiO_2

The (Fig 3) shows the hysteresis plots obtained for the as-prepared Ni and Ni/SiO_2. A comparison of the saturation magnetization values for pure and coated Ni particles in (Fig 4) indicates the presence of about ~50-wt% of Ni in the silica matrix. The high coercivity for Ni/SiO_2 is due to several possibilities. One of most likely reason is the high ratio of the non-magnetic SiO_2 in the composite can separate the Ni

RESULTS AND DISCUSSION

XRD patterns obtained for pure Ni nanoparticles as-prepared and annealed in air at 473, 573 and 673 K for 1 h are presented in (Fig 1) and the patterns for the silica coated Ni particles as-prepared and annealed at 573, 673 and 873 K for 2 h are shown in (Fig 2). The patterns correspond to diffraction from fcc-Ni. The estimated average grain size of the as-prepared Ni particles was 11 nm calculated for the (111) profile using the Scherrer formula [26]. The onset of oxidation, as revealed by the first appearance of weak NiO peaks in (Fig 1), is noticed at 573 K in the case of bare Ni nanoparticles and reaches completion at 673 K, whereas for the silica coated particles this onset occurs only at 673 K and oxidation proceeds slowly until 873 K (Fig 2). This establishes that silica coating provides increased thermal stability for these nanoparticles.

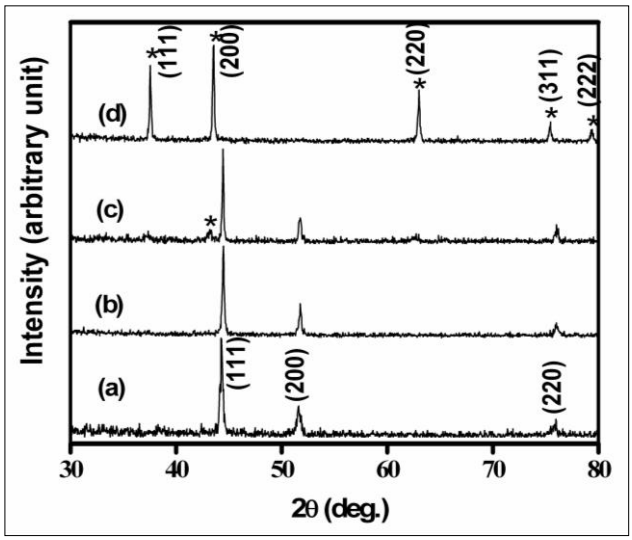

Fig 2 X-ray diffraction patterns of (a) as-prepared Ni/SiO_2 nanocomposite and annealed at (b) 573 K, (c) 673 K and (d) 873 K for two hours (in air) ∗-indicates the peaks corresponding to fcc-NiO

particles from agglomeration and hence reducing the coupling between particles. Similar result has been reported for Co/SiO_2 nanocomposite [27].

The complex impedance plane plot of as-prepared and annealed nickel-silica nanocomposites are shown in (Fig 4). The graph shows a single semicircle at high frequencies due to the silica coated nickel and an arc in the low frequency region, which is attributed to the interface polarization effect [28]. The depressed semicircular-arc can be defined by a parallel combination of resistance (R_p) and constant phase element (CPE) capacitor. The impedance of CPE is expressed as:

$$C(\omega) = B(j\omega)^{\alpha-1}$$

The parameter B is a constant for given experimental data. The exponent α gives the degree of energy dissipation and varies between 0 and 1. The impedance of CPE is purely capacitative for α = 1 and purely resistive for α =0 [29]. A non-linear least squares fitting of the high frequency data using a parallel R_p-CPE equivalent circuit yielded $7.4x10^4$ $2.2x10^5$ and $2.8x10^8$ Ωcm for the resistivities of the as prepared, annealed at 573 and 673 K samples respectively. Large resistivity for the annealed sample could mainly be due to the densification of silica around the nickel nanoparticles. The depressed semicircle observed in our sample can be explained as due to presence of surface charge states due to chemisorbed functional groups and moisture [30]. Thus, the depression of semicircle is less after annealing the sample.

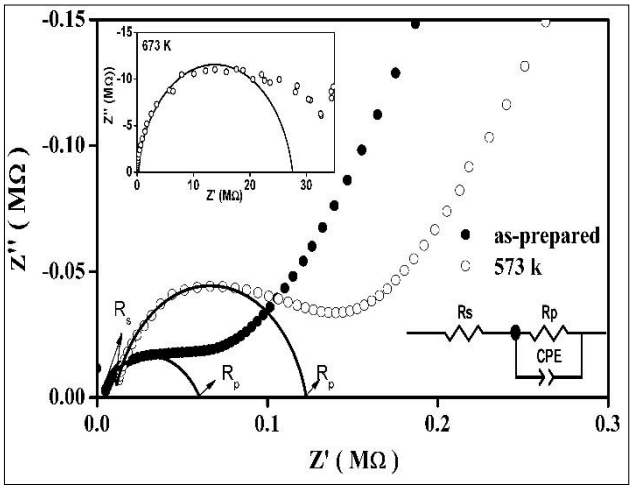

Fig 4 Z′ vs Z′′ plot for the as-prepared and annealed (at 573 K) Ni/SiO_2 nanocomposite measured at RT. Inset shows impedance plot for Ni/SiO2 sample annealed at 673 K and corresponding equivalent circuit. R_s: Ohmic serial resistance, R_p: Charge transfer resistance and CPE: Constant phase element

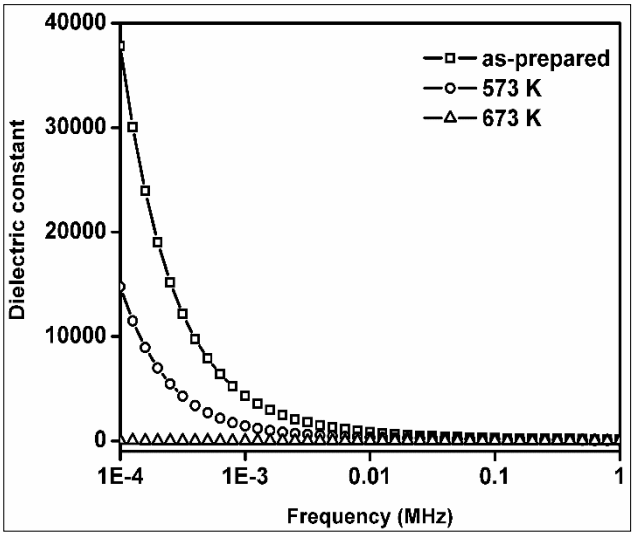

Fig 5 The real part (ε′) of the dielectric constant at RT as a function of frequency for the as-prepared and annealed samples of Ni/SiO_2

The temperature dependence of dc conductivity of as-prepared Ni/SiO_2 nanocomposite in the temperature range from 323 to 363 K were analyzed. The conductivity is found to decrease with increasing temperature. The activation energy for the thermally activated hopping process was obtained by fitting the dc conductivity data with the Arrhenius relation,

$$\sigma T = \sigma_0 \exp\left(-E_a/kT\right) \quad \ldots\ldots\ldots\ldots\ldots (1)$$

where, σ_0 is the pre-exponential factor with the dimensions of $(\Omega cm)^{-1}$ K, E_a is the activation energy for dc conductivity and k is the Boltzmann constant. The activation energy was calculated for the as-prepared Ni/SiO_2 nanocomposite as 1.31 eV. Szu *et al*. [31] have reported an activation energy of 1.04 eV for $Cu_{10}(SiO_2)_{90}$ nanocomposite.

(Fig 5) shows the variation of dielectric constant as a function of frequency for the as-prepared and the annealed nanocomposite samples. It can be seen that the dielectric constant sharply decreases as the frequency increases up to 1 kHz and stabilizes at about 840 above 10 kHz for the as prepared sample. The same behaviour is noticed even for the sample annealed at 573 K. It stabilizes even at a lower value of about 330. But the sample annealed at 673 K shows an almost frequency independent dielectric constant (34-14) from 100 Hz to 1 MHz. Further it is clear from this study that the dielectric constant decreases with increase in annealing temperature. Tepper and Berger [32] have reported a similar behaviour for the dielectric constant of silica at high frequencies although the values are much smaller. Very high dielectric constant values were reported by Pecharroman *et al*. [33] in Ni-$BaTiO_3$ cermets particularly for samples with high Ni content. They have explained this by means of a percolation threshold and demonstrated the abrupt increase in the dielectric constant at the threshold concentration from measurements of dielectric constant for various concentrations. Similar results were reported in the literature for Ni-$BaTiO_3$ nanocomposites [34]. In the present study the high dielectric constant of as-prepared and annealed at 473 K samples, may be attributed to the high nickel content (~ 50%) in the composite. Recently Nandy *et al*. [16] studied the dielectric behaviour of Ni nanoparticle in the silica matrix with 5-15% Ni concentration and reported substantial increase in the dielectric constant of the composite from 5 to 80 as the nickel content was increased to 15%. Yan et al also observed enhanced dielectric constant for SiC/Ni nanocomposites over pure SiC powder [17].

The real part of ac conductivity as a function of frequency for the as-prepared and annealed (at 573 K) Ni:SiO_2 nanocomposite samples were analyzed. The total conductivity can be written as.

$$\sigma_{total}(\omega) = \sigma_{dc} + \sigma_{ac}(\omega) \quad \ldots\ldots\ldots\ldots (2)$$

where σ_{dc} is frequency independent ($\omega = 0$) dc conductivity and $\sigma(\omega)$ is frequency dependent ac conductivity. According to Jonscher's [36] universal power law [35] the frequency dependent conductivity can in almost all cases be modeled as

$$\sigma_{ac}(\omega) = A\omega^n \quad \ldots\ldots\ldots\ldots\ldots (3)$$

where A is a constant and n ($0 < n < 1$) is the power law exponent often used to describe the ac component contributing to the dispersive region. A large value of n ($0.5 < n < 0.9$) signifies transport by hopping charge carriers. In the as-prepared as well as annealed samples, conductivity vs frequency trend shows two distinct regions, one with small slope and hence a small value for n $(n = d\log\sigma_{ac}(\omega)/d\log\omega)$ and another with a large value of n. This critical frequency of transition from low n ($n \leq 0.2$) to high n ($n > 0.5$) region is about 100 kHz for the as prepared composite and about 10 kHz for the sample annealed at 573 K and the values of n are 0.2 and 0.58 for the as-prepared sample while they are 0.18 and 0.65 for the sample annealed at 573 K. In the case of samples annealed at 673 K, the conductivity shows considerable frequency independent behaviour above 25 kHz, with a lower value for n. According to universal power law the small value of n in the low frequency region could be explained with high ratio of loss in the real part of dielectric constant ($\varepsilon'(\omega)$), since dc conductivity does not contribute to $\varepsilon'(\omega)$.

CONCLUSION

Nanocrystalline fcc-Ni particles were synthesized and successfully coated with silica. TEM images confirmed the nanoparticulate nature of the composite. XRD studies show the increased thermal stability of silica coated nickel nanoparticles. Magnetic hysteresis and EDAX analyses of the composite indicate an Ni:SiO_2 ratio of 1:1. The ac conductivity measurement reveals a frequency dependent behaviour broadly consistent with Jonsher's universal law for the conductivity of the silica coated nickel nanoparticles. A large dielectric

constant observed for the composite is probably due to a large volume fraction of nickel nanoparticles in silica matrix.

Acknowledgments

The work was supported by a Research Facilities of Department of Nuclear Physics, University of Madras. The authors are acknowledging Research Scholars and Technical staff members of Department of Physics for their support.

LITERATURE CITED

1. Chen Y, Peng DL, Lin D, Luo X. 2007. Preparation and magnetic properties of nickel nanoparticles via the thermal decomposition of nickel organometallic precursor in alkylamines. *Nanotechnology* 18: 505703.
2. He L, Zheng W, Zhou W, Du H, Chen C, Guo L. 2007. Size-dependent magnetic properties of nickel nanochains. *Jr. Phys.: Condens. Matter*. 19: 036216.
3. Zamorskiia MK, Nounehb K, Kobayashic K, Oyamac M, Ebothed J, Reshak AH. 2008. Acoustically induced light gyration in nickel nanoparticles. *Optics and Laser Technology* 40(3): 499-504.
4. Liu CC, Lue JT. 2007. Physical properties of nanomaterials. *Optics Communications* 280: 477.
5. Joo J, Lee SJ, Park DH, Kim YS, Lee Y, Lee CJ, Lee SR. 2006. Field emission characteristics of electrochemically synthesized nickel nanowires with oxygen plasma post-treatment. *Nanotechnology* 17: 3506.
6. Rinaldi A, Peralta P, Friesen C, Sieradzki K. 2008. Sample-size effects in the yield behavior of nanocrystalline nickel. *Acta Materialia* 56: 511-517.
7. Kim JS, Kuk E, Yu KN, Kim JH, Park SJ, Lee HJ, Kim SH, Park YK, Park YH, Hwang CY, Kim YK, Lee YS, Jeong DH, Cho MH. 2007. Antimicrobial effects of silver nanoparticles. *Nanomedicine* 3(1): 95-101.
8. Pan YX, Liu CJ, Shi P. 2008. Preparation and characterization of coke resistant Ni/SiO2 catalyst for carbon dioxide reforming of methane. *Journal of Power Sources* 176: 46-53.
9. Liu G, Li Y, Chu W, Shi X, Dai X, Yin Y. 2008. Plasma-assisted preparation of Ni/SiO_2 catalyst using atmospheric high frequency cold plasma jet. *Catal. Commun.* 9: 1087-1091.
10. Das S, Panda SK, Nandi P, Chaudhuri S, Pandey A, Ranganathan R. 2007. Sol–gel synthesized SnO_2 nanoparticles and their properties. *Jr. Nanosci. Nanotechnology* 7: 4402-4411.
11. Cao Y, Cao J, Zheng M, Liu J, Ji G, Ji H. 2007. Facile fabrication of magnetic nanocomposites of ordered mesoporous carbon decorated with nickel nanoparticles. *Jr. Nanosci. Nanotechnology* 7: 504-509.
12. Tomita S, Jönsson PE, Akamatsu K, Nawafune H, Takayama H. 2007. Tuning magnetic interactions in ferromagnetic-metal nanoparticle systems. *Phys. Rev. B* 76: 174432.
13. Sun Y, Sun J, Liu M, Chen Q. 2007. Mechanical strength of carbon nanotube-nickel nanocomposites. *Nanotechnology* 18: 505704.
14. Yeshchenko OA, Dmitruk IM, Alexeenko AA, Dmytruk AM. 2008. Optical properties of sol–gel fabricated Ni/SiO_2 glass nanocomposites. *Jr. Phys. Chem. Solids* 69: 1615-1622.
15. Amekura H, Takeda Y, Kishimoto N. 2004. Magneto-optical Kerr spectra of nickel nanoparticles in silica glass fabricated by negative-ion implantation. *Thin Solid Films* 464/465: 268-272.
16. Nandy S, Mallick S, Ghosh PK, Das GC, Mukherjee S, Mitra MK, Chattopadhyay KK. 2008. Impedance spectroscopic studies of nickel nanocluster in silica matrix synthesized by sol–gel method. *Journal of Alloy Compounds* 453: 1-2.
17. Yan Z, Yu-Qing K, Xiao-Yong F, Jie Y, Xiao-Ling S, Wei-Li S, Mao-Sheng C. 2008. Mechanism of enhanced dielectric properties of SiC/Ni Nanocomposites. *Chin. Phys. Letters* 25(5): 1902.
18. Fonseca FC, Goya GF, Jardim RF, Muccillo R, Carreño NLV, Longo E, Leite ER. 2002. Superparamagnetism and magnetic properties of Ni nanoparticles embedded in SiO_2. *Phys. Rev*. B 66: 104406.
19. Fu W, Yang H, Chang L, Li M, Bala H, Yu Q, Zou G. 2005. *Colloids and Surfaces A: Physicochem. Eng. Aspects*. 262: 71.
20. Iwamoto M, Kosugi Y. 2007. Highly selective conversion of ethene to propene and butenes on nickel ion-loaded mesoporous silica catalysts. *Jr. Phys. Chem. C*. 111L: 13-15.
21. Tang NJ, Zhong W, Liu W, Jiang HY, Wu XL, Du YW. 2004. Synthesis and complex permeability of Ni/SiO_2 nanocomposite. *Nanotechnology* 15: 1756.
22. Liu ZW, Phua LX, Liu Y, Ong CK. 2006. Microwave characteristics of low density hollow glass microspheres plated with Ni thin-film. *Jr. Applied Physics* 100: 093902.
23. Peng K, Zhoua L, Hu A, Tang Y, Li D. 2008. Synthesis and magnetic properties of $Ni–SiO_2$ nanocomposites. *Mater. Chem. Physics* 111: 34-37.
24. Chen DH, Hsieh CH. 2002. Synthesis of nickel nanoparticles in aqueous cationic surfactant solutions. *Journal of Materials Chemistry* 12: 2412-2415.
25. Li Z, Han C, Shen J. 2006. Reduction of Ni^{2+} by hydrazine in solution for the preparation of nickel nano-particles. *Journal of Materials Sciences* 41: 3473-3480.
26. Stöber W, Fink A, Bohn E. 1968. Controlled growth of monodisperse silica spheres in the micron size range. *Jr. Colloid Interface Science* 26: 62-69.
27. Scherrer P, Gottinger. 1918. Nachrichten von der Gesellschaft der Wissenschaften zu Göttingen, Mathematisch-Physikalische Klasse. *Nachrich* 2: 98-100.
28. Mishra SR, Dubenko L, Losby J, Marasinghe K, Mehdi Ali, Ali N. 2005. Magnetic properties of magnetically soft nanocomposite $Co–SiO_2$ prepared via mechanical milling. *Jr. Nanosci. Nanotechnology* 5(12): 2082-2087.
29. Villegas MA, Jurado LR, Navarro FJM. 1989. Dielectric properties of $R_2O–SiO_2$ glasses prepared via sol-gel. *Journal Mater. Science* 24: 2884-2890.
30. Macdonald JR. 1987. *Impedance Spetroscopy*. New York, Wiley.
31. Ahmad MM, Makhlouf SA, Khalil KMS. 2006. Dielectric behavior and ac conductivity study of NiO/Al_2O_3 nanocomposites in humid atmosphere. *Journal of Applied Physics* 100: 094323.

32. Szu SP, Lin CY. 2003. AC impedance studies of copper doped silica glass. *Materials Chemistry and Physics* 82: 295-300.
33. Tepper T, Berger S. 1999. Correlation between microstructure, particle size, dielectric constant, and electrical resistivity of nano-size amorphous SiO_2 powder. *Nanostruct. Mater.* 11:1081-1089.
34. Pecharroman C, Esteban-Betegon F, Bartolome JF, Lopez-Esteban S, Moya JS. 2001. New Percolative $BaTiO_3$–Ni Composites with a High and Frequency-Independent Dielectric Constant ($\epsilon_r \approx 80000$). *Advanced Materials* 13: 1541-1544.
35. Chena R, Wang X, Wen H, Li L, Gui Z. 2004. Enhancement of dielectric properties by additions of Ni nano-particles to a X7R-type barium titanate ceramic matrix. *Ceramics International* 30(7): 1271-1274.
36. Jonscher K. 1977. The 'universal' dielectric response. *Nature* 267: 673-679.
37. Singh GP, Ram S. 2008. Silver-modified CrO_2 of core–shell nanoparticles and their magnetic and impedance properties. *Jr. Am. Ceram. Society* 91: 322-324.